

### Adsorption of Benzene and Methyl-Substituted Benzenes at the Vapor/Water Interface. 3. Finite Binary-Component VHOC Adsorption

Robert G. Bruant, Jr. and Martha H. Conklin\*

Department of Hydrology and Water Resources, The University of Arizona, P.O. Box 210011, Harshbarger Building 11, Tucson, Arizona 85721-0011

Received: August 17, 2000; In Final Form: December 21, 2000

Isothermal measurements (285.2, 291.2, and 298.2 K) of equilibrium aqueous solution surface tension (pressure) as a function of partial vapor-phase volatile hydrophobic organic compound (VHOC) pressure for benzene/methylbenzene, benzene/1,2-dimethylbenzene, benzene/1,3-dimethylbenzene, benzene/1,4-dimethylbenzene, and benzene/1,3,5-trimethylbenzene binary mixture pairs were made employing pendant drop tensiometry and gas chromatographic analysis. Surface pressure isotherms were developed at atmospheric pressure at three intermediate constant mole ratios for each compound pair and experimental temperature, from zero to near/at total VHOC (i.e., solute) saturated vapor pressure. Corresponding single-solute surface pressure isotherms were also measured. Analyses indicate that vapor-phase/interface-phase binary VHOC equilibrium is well described by ideal mixing equations applied to single-component surface pressure and relative interface excess isotherms. The interface phase was found to be enriched with respect to the larger molecular size components (i.e., methyl-substituted benzenes) for a given vapor-phase composition, in a manner very similar to vapor-phase/organic liquid-phase partitioning.

#### Introduction

Volatile hydrophobic organic compounds (VHOCs), commonly derived from petroleum products and industrial solvents, are pervasive environmental contaminants. While discharges of these compounds commonly involve multiple interacting species, which have been considered in terms of bulk environmental phases (e.g., refs 1–3), solute mixture behavior at the vapor/water interface has not been addressed. Such neglect is assumed, in part, due to the experimental difficulties in confining and quantifying vapor/water interface behavior of these high vapor pressure, sparsely soluble organic compounds. As a result, in environmental systems where the magnitude of the vapor/water interface imparts a significant sink for VHOCs (e.g., unsaturated groundwater systems, atmospheric water droplets and aerosols, and adsorptive bubble remediation techniques),<sup>4</sup> there is little understanding of the associations between adsorbed components and the magnitude of interface adsorption.

The goal of this study is to define, both experimentally and theoretically, binary VHOC equilibrium between the vapor phase and vapor/water interface phase. Aqueous solution surface tension as a function of single and binary component vapor-phase VHOC (i.e., solute) pressure isotherms for benzene/methylbenzene (MB), benzene/1,2-dimethylbenzene (12DMB), benzene/1,3-dimethylbenzene (13DMB), benzene/1,4-dimethylbenzene (14DMB), and benzene/1,3,5-trimethylbenzene (135-TMB) pairs were measured experimentally at atmospheric pressure using pendant drop tensiometry, gas chromatographic analysis, and a dynamic adsorption protocol. Component and pair selection were based on three factors: (1) the compounds are common environmental contaminants, (2) the homologous suite allows a systematic analysis of solute structure on resulting interfacial behavior, and (3) the mixture behavior in the vapor

phase and organic liquid phase is relatively ideal (considered an appropriate starting point for analysis of VHOC mixture adsorption).

Three intermediate constant vapor-phase mole ratio (i.e., molar ratio of VHOC components, neglecting air and water vapor) surface tension isotherms, in addition to single solute isotherms, were measured for each solute pair at temperatures of 285.2, 291.2, and 298.2 K for total vapor-phase VHOC pressures ranging from zero to near/at saturated vapor pressure. Isotherms (converted to surface pressure for quantitative treatment and presentation) were interpolated with a mathematical form combining a nonideal two-dimensional equation of state and the Gibbs relative interface excess equation to determine isothermal interface-phase VHOC adsorption. Equilibrium between vapor-phase and interface-phase VHOCs was analyzed in terms of an ideal solution model applied to single component VHOC surface pressure isotherms. Predicted mixing was compared to measured intermediate mole ratio surface pressure measurements, and corresponding relative interface excess determinations, to address the suitability of the ideal mixing interpretation.

#### Theory

**Vapor/Interface Mixing.** The ideal equilibrium relationship between vapor-phase (V) and vapor/water interface-phase (I) VHOC mixture composition at constant surface pressure and temperature is defined as<sup>5–11</sup>

$$z_i^V p_T^V = Z_i^I p_i^{V,\text{pure}} \quad i = 1, 2 \quad (1)$$

where  $z_i^V$  is the vapor-phase VHOC mole ratio (neglecting air and water vapor) [unitless],  $p_T^V$  is the total vapor-phase VHOC pressure [Pa],  $Z_i^I$  is the interface-phase VHOC mole ratio (neglecting air and water) [unitless],  $p_i^{V,\text{pure}}$  is the total vapor-

\* Corresponding author. E-mail: martha@hwr.arizona.edu.; Telephone: 520-621-5829. Fax: 520-621-1422.

phase VHOC pressure of the single solute ( $\equiv p_T^V$  when  $z_i^V = 1$ ) [Pa], and  $i$  refers to solute components 1 and 2 (for the presented analysis, benzene is defined as component 1 (i.e., VHOC1) and the individual methyl-substituted benzenes are defined as component 2 (i.e., VHOC2)). Parameters  $z_i^V$  and  $Z_i^I$  are explicitly defined as

$$z_i^V = p_i^V/p_T^V \quad i = 1, 2 \quad (2)$$

$$Z_i^I = \Gamma_i/\Gamma_T \quad i = 1, 2 \quad (3)$$

where

$$p_T^V = \sum_{i=1}^2 p_i^V \quad (4)$$

$$\Gamma_T = \sum_{i=1}^2 \Gamma_i \quad (5)$$

$p_i^V$  is the partial vapor-phase VHOC pressure [Pa],  $\Gamma_i$  is the partial relative solute interface excess per unit surface area (with the interface excess of solvent equal to zero and neglecting air) [mol m<sup>-2</sup>], and  $\Gamma_T$  is the corresponding total relative solute interface excess [mol m<sup>-2</sup>].

Writing eq 1 in terms of the total vapor-phase solute pressure and vapor-phase mole ratio of solute component 2, the total vapor-phase solute pressure and interface-phase mole ratio of solute component 2, and the interface-phase mole ratio and vapor-phase mole ratio of solute component 2 gives, respectively,

$$p_T^V = p_1^{V,\text{pure}} p_2^{V,\text{pure}}/[p_2^{V,\text{pure}} + z_2^V(p_1^{V,\text{pure}} - p_2^{V,\text{pure}})] \quad (6)$$

$$p_1^V = p_1^{V,\text{pure}} - Z_2^I(p_1^{V,\text{pure}} - p_2^{V,\text{pure}}) \quad (7)$$

$$Z_2^I = p_1^{V,\text{pure}}/(p_1^{V,\text{pure}} + p_2^{V,\text{pure}}/z_2^V - p_2^{V,\text{pure}}) \quad (8)$$

If eq 6 fits decomposition of the aqueous solution surface pressure data (i.e., defining total vapor-phase VHOC pressure as a function of vapor-phase VHOC2 mole ratio at constant surface pressure), then solute-solute mixing is considered ideal within both phases. For such a situation, the interface-phase mole ratios are defined solely in terms of measurement of single-component surface pressure isotherms from eqs 7 and 8. Partial relative solute interface excess can then be determined for any interface-phase VHOC mole ratio from single component relative interface excess (at constant temperature and surface pressure):

$$1/\Gamma_T = \sum_{i=1}^2 Z_i^I/\Gamma_i^{\text{pure}} \quad (9)$$

where  $\Gamma_i^{\text{pure}}$  is the total relative VHOC interface excess for single solute adsorption ( $\equiv \Gamma_T$  when  $Z_i^I = 1$ ) [mol m<sup>-2</sup>].

**Data Interpolation.** To define finite VHOC adsorption, the experimental aqueous solution surface pressure versus total vapor-phase VHOC pressure isotherms are interpolated using a combined form of a nonideal two-dimensional equation of state and the Gibbs relative interface excess equation. The equation of state is defined as

$$\pi(a - a^0) = RT \quad (10)$$

where  $\pi$  is the aqueous solution surface pressure (surface tension of solute-free water less measured aqueous solution surface tension) [N m<sup>-1</sup>],  $a$  is the molecular area projection (single solute adsorption) or average molecular area projection (binary solute adsorption) [m<sup>2</sup> mol<sup>-1</sup>],  $a^0$  is an empirical fitting constant [m<sup>2</sup> mol<sup>-1</sup>],  $R$  is the molar gas constant [J mol<sup>-1</sup> K<sup>-1</sup>], and  $T$  is the absolute temperature [K].<sup>12-15</sup>

For the current experimental procedure and analysis of binary solute equilibrium, where vapor-phase VHOC mole ratios are held constant over the vapor-phase VHOC pressures considered for each surface pressure isotherm, total solute interface excess is given by the Gibbs equation as<sup>6,10,16-18</sup>

$$\Gamma_T = (1/RT)(d\pi/d\ln p_T^V) \quad (11)$$

Total relative VHOC interface excess for single solute adsorption is defined in an analogous manner:

$$\Gamma_i^{\text{pure}} = (1/RT)(d\pi/d\ln p_i^{\text{pure}}) \quad (12)$$

Combining, independently, eq 11 (where  $a = 1/\Gamma_T$ ) and eq 12 (where  $a = 1/\Gamma_i^{\text{pure}}$ ) with eq 10 and integrating gives the resulting equation of surface pressure:

$$p_T^V \text{ or } p_i^{V,\text{pure}} = \pi \exp(\pi a^0/RT + c) \quad (13)$$

where  $c$  is an integration constant [unitless]. The given equation was fit to the experimental data using a nonlinear least-squares regression routine to define values for  $a^0$  and  $c$ . To approximate the total relative solute interface excess for each measurement of surface tension (pressure), eq 10 was rearranged, incorporating the interpolated  $a^0$  values from eq 13:

$$\Gamma_T \quad \text{or} \quad \Gamma_i^{\text{pure}} = (RT/\pi + a^0)^{-1} \quad (14)$$

## Materials and Methods

**Chemicals.** Benzene (C<sub>6</sub>H<sub>6</sub>, ≥99.5%), methylbenzene ([CH<sub>3</sub>]-C<sub>6</sub>H<sub>5</sub>, ≥99.5%), 1,2-dimethylbenzene (1,2-[CH<sub>3</sub>]<sub>2</sub>C<sub>6</sub>H<sub>4</sub>, ≥99%), 1,3-dimethylbenzene (1,3-[CH<sub>3</sub>]<sub>2</sub>C<sub>6</sub>H<sub>4</sub>, ≥99%), 1,4-dimethylbenzene (1,4-[CH<sub>3</sub>]<sub>2</sub>C<sub>6</sub>H<sub>4</sub>, ≥99%), and 1,3,5-trimethylbenzene (1,3,5-[CH<sub>3</sub>]<sub>3</sub>C<sub>6</sub>H<sub>3</sub>, ≥99%) were purchased from Fluka Chemical (Ronkonkoma, NY) and used without further refinement. Water from a Millipore deionization system was distilled at atmospheric pressure in a potassium permanganate/sodium hydroxide solution followed by all-water distillation; liquids were assumed to have equilibrium concentrations of atmospheric air. Relevant physicochemical properties of the compounds were obtained from Daubert and Danner.<sup>19</sup>

**Experimental System.** Detail of the experimental system is presented elsewhere<sup>20,21</sup> and only a brief summary (with extension to binary VHOC analysis) is currently given. Aqueous solution surface tension measurements were made at atmospheric pressure using pendant drop tensiometry and axisymmetric drop shape analysis-profile (ADSA-P) (Applied Surface Thermodynamics Research Associates, Toronto, Ontario).<sup>22,23</sup> Drops were formed from a Teflon capillary inside a gastight stainless steel environmental cell, with temperature regulated to ±0.2 K. Pendant drops were illuminated by a halogen light source and imaged using a charge-coupled device (CCD) video camera.

Gas-washing bottles (Chemglass, Vineland, NJ) were used to contact advecting air with both liquid water and liquid organic phases for vapor delivery to the environmental cell. For binary solute experiments, organics were mixed in a single bottle at organic liquid-phase mole fractions to give intermediate vapor-

phase VHOC mole ratios (i.e., mole ratios between 0 and 1) determined by Raoult's law relationships. Liquid-phase mixing and large organic liquid-phase reservoirs (minimizing the influence of volatile losses on vapor-phase/liquid-phase ratios) allowed constant vapor-phase VHOC mole ratios throughout the entire vapor-phase VHOC pressure ranges considered for each measured surface tension (pressure) isotherm. An electronically actuated sample loop was attached at the immediate environmental cell outlet for automated sampling of the advecting air/vapor phase. Samples were delivered directly through fused-silica tubing to a Varian 3600CX gas chromatograph (GC) with flame ionization detector (FID) for determination of vapor-phase VHOC pressures.

**Measurement Protocol.** Experiments were initiated by forming a solute-free pendant water drop in contact with advecting humidified air. After thermal and mechanical equilibration of the water drop, solute delivery was switched to the environmental cell. Simultaneously, automated image acquisition and sample injection to the GC were initiated, with measurements made at 120 s intervals. Aqueous solution surface tensions and GC peak areas were continuously monitored to determine when minimum and maximum values were reached, respectively (always less than  $3.6 \times 10^4$  s).

Aqueous solution surface tension measurements were matched to total vapor-phase VHOC pressures for each analysis time (i.e., rapid equilibration between interface and vapor phases, cf. refs 20 and 21) to generate individual surface tension (pressure) isotherm coordinates. Vapor-phase VHOC mole ratios were calculated for each analysis time (i.e., for each measured vapor-phase solute pressure pair) and averaged (arithmetic mean) over the entire measured vapor-phase solute pressure range to define the mean mole ratio and one standard deviation for each binary solute aqueous solution surface tension (pressure) isotherm.

Surface tension (pressure) isotherms were measured for single VHOC adsorption at 287.2, 291.2, and 298.2 K. Isotherms were measured at three intermediate vapor-phase VHOC mole ratios for benzene/MB, benzene/12DMB, benzene/13DMB, benzene/14DMB, and benzene/135TMB mixtures at the same temperatures.

## Results

An illustration of raw measurements of aqueous solution surface tension and vapor-phase VHOC pressure for the benzene/MB solute pair at 285.2 K is given in Figure 1. The ability of the system to quantify both partial and total vapor-phase solute pressures, in addition to the concurrent decrease in aqueous surface tension with increasing vapor-phase VHOC pressure, is apparent. Corresponding partial vapor-phase pressure of MB as a function of partial vapor-phase pressure of benzene is given in Figure 2. The strong linearity of the relationship is clear, imparting very constant mole ratios over the vapor-phase solute pressure ranges considered.

Measurement conditions/results for all binary solute experiments, including experiment number, temperature, number of measured points per isotherm, and fraction of isotherm measured (i.e., the maximum measured total vapor-phase solute pressure  $p_{T,\max}^V$  divided by the total solute mixture saturated vapor pressure  $p_{T,\text{sat}}^V$ ), are provided in Table 1. Mean vapor-phase solute mole ratios (used as a lumped description of the mole ratio for each complete surface pressure isotherm) and standard deviations are given in Table 2. Results for single component surface pressure isotherm measurements are presented in Table 3 (fractions of isotherms measured were calculated from the

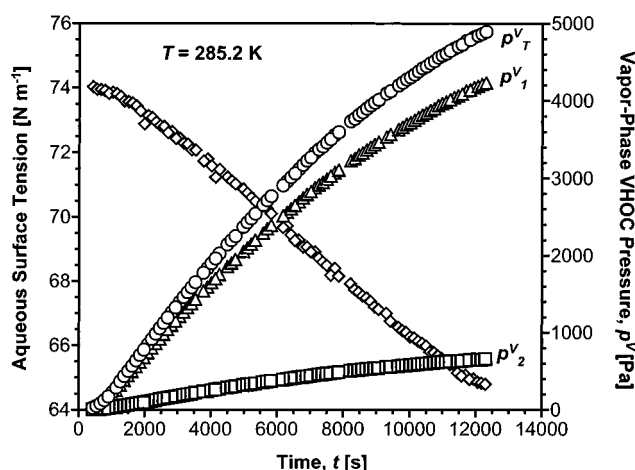


**Figure 1.** Raw experimental output for the benzene/MB mixture experiment at 285.2 K and mean MB vapor-phase mole ratio  $z_2^V$  of  $1.32 \times 10^{-1}$ : Aqueous solution surface tension ( $\diamond$ ), partial vapor-phase benzene pressure  $p_1^V$  ( $\Delta$ ), partial vapor-phase MB pressure,  $p_2^V$  ( $\square$ ), and total vapor-phase benzene/MB pressure  $p_T^V$  ( $\circ$ ).

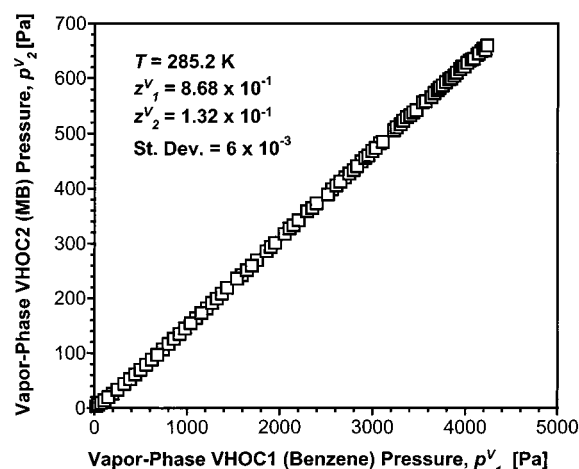


**Figure 2.** Partial vapor-phase MB pressure  $p_2^V$  as a function of partial vapor-phase benzene pressure  $p_1^V$  for the benzene/MB mixture experiment (Figure 1) at 285.2 K and mean MB vapor-phase mole ratio  $z_2^V$  of  $1.32 \times 10^{-1}$ .

maximum measured vapor-phase solute pressure  $p_{i,\max}^{V,\text{pure}}$  divided by the single solute saturated vapor pressure  $p_{i,\text{sat}}^{V,\text{pure}}$ ).

Figure 3 presents the five measured isotherms of aqueous solution surface pressure as a function of total vapor-phase solute pressure for the benzene/14DMB pair at 298.2 K. The data are present logarithmically with respect to the total vapor-phase VHOC pressure axis to highlight the distinct separation between isotherms as a function vapor-phase VHOC mole ratio and the regularly changing shape between the single component surface pressure isotherms. For all isotherms, as the mean vapor-phase VHOC2 mole ratio  $z_2^V$  increases, there is a greater change in aqueous solution surface tension for a given total vapor-phase VHOC pressure  $p_T^V$ .

To convey the variation in surface pressure isotherm shape as a function of solute pair considered, isotherms are presented in Figure 4 for benzene/MB, benzene/14DMB, and benzene/135TMB pairs at 285.2 K and vapor-phase VHOC2 mole ratio of approximately  $1 \times 10^{-1}$  (i.e.,  $1.32 \times 10^{-1}$ ,  $9.3 \times 10^{-2}$ , and  $9.9 \times 10^{-2}$ , respectively). Isotherms are concave to the surface pressure axis and exhibit monotonic increases in surface pressure as total vapor-phase VHOC pressure increases, with no limiting value of adsorption realized. It is apparent that, as the molecular

TABLE 1: Measured Isotherm Characteristics and Results of Equation 13 Fits for Binary VHOC Mixture Experiments

VHOC mixture	experiment	$T$ [K]	$n^a$	fraction measured $p_{T,\max}^V p_{T,\text{sat}}^{V-1}$	eq 13 parameters		$R^{2b}$
					$a^0 \times -10^{-5} [\text{m}^2 \text{mol}^{-1}]$	$c \times 10^{-1} [\text{unitless}]$	
B <sup>c</sup> (1 <sup>d</sup> )/MB (2)	B/MB1	285.2	57	0.964	1.23	1.29	0.997
	B/MB2	285.2	118	0.940	1.80	1.35	0.997
	B/MB3	285.2	90	0.982	1.36	1.37	0.998
	B/MB4	291.2	80	0.977	1.68	1.34	0.996
	B/MB5	291.2	164	0.944	1.40	1.37	0.998
	B/MB6	291.2	124	1.00	0.873	1.38	0.999
	B/MB7	298.2	124	1.00	1.47	1.36	0.999
	B/MB8	298.2	140	1.00	1.55	1.40	0.996
	B/MB9	298.2	158	0.991	1.35	1.43	0.998
B (1)/12DMB (2)	B/1,2-DMB1	285.2	73	0.965	2.76	1.22	0.990
	B/1,2-DMB2	285.2	55	0.935	3.08	1.27	0.991
	B/1,2-DMB3	285.2	53	0.930	2.95	1.33	0.995
	B/1,2-DMB4	291.2	73	0.962	2.32	1.23	0.996
	B/1,2-DMB5	291.2	70	0.972	2.70	1.29	0.996
	B/1,2-DMB6	291.2	55	0.948	2.52	1.34	0.995
	B/1,2-DMB7	298.2	126	0.994	1.75	1.26	0.995
	B/1,2-DMB8	298.2	127	0.957	2.78	1.33	0.996
	B/1,2-DMB9	298.2	102	1.00	2.43	1.39	0.994
B (1)/13DMB (2)	B/1,3-DMB1	285.2	58	0.895	2.05	1.20	0.991
	B/1,3-DMB2	285.2	71	0.926	2.29	1.27	0.996
	B/1,3-DMB3	285.2	48	0.901	2.23	1.32	0.993
	B/1,3-DMB4	291.2	65	0.883	2.43	1.25	0.993
	B/1,3-DMB5	291.2	73	0.957	0.994	1.24	0.996
	B/1,3-DMB6	291.2	61	0.931	1.64	1.33	0.994
	B/1,3-DMB7	298.2	143	0.917	0.735	1.22	0.999
	B/1,3-DMB8	298.2	143	0.922	1.03	1.28	0.994
	B/1,3-DMB9	298.2	113	0.932	1.07	1.34	0.994
B (1)/14DMB (2)	B/1,4-DMB1	285.2	61	0.865	2.55	1.23	0.994
	B/1,4-DMB2	285.2	65	0.901	2.25	1.29	0.993
	B/1,4-DMB3	285.2	67	0.928	2.05	1.36	0.998
	B/1,4-DMB4	291.2	90	0.908	1.58	1.24	0.998
	B/1,4-DMB5	291.2	82	0.917	2.20	1.31	0.996
	B/1,4-DMB6	291.2	80	0.942	1.67	1.36	0.993
	B/1,4-DMB7	298.2	141	0.911	1.83	1.29	0.997
	B/1,4-DMB8	298.2	181	0.980	1.47	1.33	0.999
	B/1,4-DMB9	298.2	160	0.967	1.64	1.40	0.999
B (1)/135TMB (2)	B/1,3,5-TMB1	285.2	81	0.911	4.20	1.17	0.988
	B/1,3,5-TMB2	285.2	50	0.876	3.72	1.22	0.986
	B/1,3,5-TMB3	285.2	59	0.880	4.04	1.30	0.977
	B/1,3,5-TMB4	291.2	111	0.934	3.62	1.20	0.994
	B/1,3,5-TMB5	291.2	90	0.881	3.85	1.25	0.992
	B/1,3,5-TMB6	291.2	90	0.894	2.38	1.29	0.997
	B/1,3,5-TMB7	298.2	194	0.926	3.23	1.22	0.996
	B/1,3,5-TMB8	298.2	225	0.942	4.25	1.30	0.990
	B/1,3,5-TMB9	298.2	194	0.973	3.93	1.36	0.993

<sup>a</sup> Number of data points. <sup>b</sup> Coefficient of determination. <sup>c</sup> B  $\equiv$  benzene. <sup>d</sup> (1) indicates VHOC1, (2) indicates VHOC2.

size of component 2 increases, there is a greater change in aqueous solution surface tension for a given total vapor-phase VHOC pressure and temperature. Due to the lower volatility of the greater molecular size compounds, the absolute change in aqueous solution surface tension is lower near/at total saturated vapor pressure. Results of surface pressure isotherm interpolations using eq 13 for binary and single solute adsorption are presented in Tables 1 and 3, respectively.

## Discussion

**Constant Surface Pressure Data.** To apply the equilibrium relationship defined by eq 6, the five aqueous solution surface pressure isotherms for each mixture pair and temperature were decomposed at constant surface pressure ( $1 \times 10^{-3} \text{ N m}^{-1}$  intervals) to define the dependence between total vapor-phase VHOC pressure and vapor-phase component 2 mole ratio. Figure 5 presents the decomposition as a function of constant surface pressure ( $1 \times 10^{-3}$ ,  $3 \times 10^{-3}$ , and  $7 \times 10^{-3} \text{ N m}^{-1}$  presented) for the benzene/13DMB pair at 285.2 K. Individual chart symbols represent values derived from experimental

surface pressure isotherm results; error bars (barely visible) represent the associated mean vapor-phase VHOC pressure mole ratio standard deviations. The data, in general, exhibit a convex downward curvature, indicating that the adsorption is dominated by the larger molecular size compound (i.e., 13DMB).<sup>6</sup> The trends of the data tend to become steeper at higher values of constant surface pressure, showing that relationships between total vapor-phase VHOC pressure and mean vapor-phase mole ratio are significantly dependent on the surface pressure of the system.

Figure 6 provides illustration of the temperature dependence on the decomposed data sets at constant surface pressure of  $4 \times 10^{-3} \text{ N m}^{-1}$  for the benzene/135TMB solute pair. Similar to that noted in Figure 5, the apparent curvature of the derived data tends to become steeper with increasing temperature. To show the dependence of the experimental data on solute type, decomposed results for benzene/MB, benzene/13DMB, and benzene/135TMB are presented in Figure 8 at constant surface pressure of  $3 \times 10^{-3} \text{ N m}^{-1}$  at 285.2 K. Distinct trends as a function of mixture composition are apparent, with more



**TABLE 2: Mean Vapor-Phase Solute Mole Ratios and Standard Deviations for Binary VHOC Mixture Experiments**

VHOC mixture	experiment	measured vapor-phase VHOC mole ratios		
		mean $z_1^V \times 10^1$	mean $z_2^V \times 10^1$	SD $\times 10^2$ <sup>a</sup>
B <sup>b</sup> (1 <sup>c</sup> )/MB (2)	B/MB1	2.27	7.73	0.4
	B/MB2	6.84	3.16	1.2
	B/MB3	8.68	1.32	0.6
	B/MB4	2.10	7.90	0.7
	B/MB5	6.44	3.56	1.6
	B/MB6	8.40	1.60	1.2
	B/MB7	2.02	7.98	1.0
	B/MB8	6.17	3.83	1.4
	B/MB9	8.35	1.65	0.6
B (1)/12DMB (2)	B/1,2-DMB1	4.07	5.93	2.9
	B/1,2-DMB2	6.54	3.46	2.7
	B/1,2-DMB3	8.50	1.50	3.0
	B/1,2-DMB4	3.74	6.26	7.0
	B/1,2-DMB5	6.18	3.82	3.5
	B/1,2-DMB6	8.13	1.87	5.6
	B/1,2-DMB7	3.49	6.51	2.5
	B/1,2-DMB8	6.40	3.60	5.0
	B/1,2-DMB9	8.33	1.67	2.1
B (1)/13DMB (2)	B/1,3-DMB1	3.80	6.20	2.0
	B/1,3-DMB2	6.62	3.38	1.2
	B/1,3-DMB3	8.69	1.31	1.5
	B/1,3-DMB4	3.47	6.53	1.7
	B/1,3-DMB5	6.27	3.73	2.5
	B/1,3-DMB6	8.43	1.57	1.2
	B/1,3-DMB7	3.39	6.61	1.7
	B/1,3-DMB8	6.29	3.71	2.2
	B/1,3-DMB9	8.43	1.57	1.2
B (1)/14DMB (2)	B/1,4-DMB1	3.69	6.31	2.4
	B/1,4-DMB2	7.07	2.93	3.6
	B/1,4-DMB3	9.07	0.93	1.5
	B/1,4-DMB4	3.34	6.66	1.9
	B/1,4-DMB5	6.77	3.23	2.2
	B/1,4-DMB6	8.75	1.25	3.8
	B/1,4-DMB7	3.24	6.76	1.1
	B/1,4-DMB8	6.52	3.48	1.8
	B/1,4-DMB9	8.80	1.20	1.2
B (1)/135TMB (2)	B/1,3,5-TMB1	5.31	4.69	2.9
	B/1,3,5-TMB2	7.69	2.31	1.4
	B/1,3,5-TMB3	9.01	0.99	3.1
	B/1,3,5-TMB4	5.00	5.00	1.4
	B/1,3,5-TMB5	7.33	2.67	2.2
	B/1,3,5-TMB6	8.85	1.15	1.1
	B/1,3,5-TMB7	4.55	5.45	2.2
	B/1,3,5-TMB8	7.10	2.90	2.5
	B/1,3,5-TMB9	8.61	1.39	1.1

<sup>a</sup> Standard deviation. <sup>b</sup> B = benzene. <sup>c</sup> (1) indicates VHOC1, (2) indicates VHOC2.

apparent curvature for solute pairs with greater disparity between end-member molecular sizes.

**Equilibrium Mixing.** Mixture functions, derived from application of eq 6 to single-component VHOC surface pressure isotherm measurements, are illustrated in Figures 5–7 (given as the solid curves). Inspection of the agreement, both visually and quantitatively, indicates that eq 6 provides a good description of the experimental mixture data. In most cases, coefficients of determination are greater than  $9.7 \times 10^{-1}$ . Such agreement is indicative of ideal interface-phase solute–solute interactions for the VHOCs considered (assuming an ideal vapor-phase). Ideal vapor/water interface-phase behavior has also been noted for mixtures of homologous nonionic surfactants.<sup>6,8,10,16,24</sup>

It is relevant to note, however, that lesser conformity between eq 6 and the experimental data for the benzene/13DMB pair (298.2 K) and benzene/MB pair (all temperatures) is noted ( $R^2 = 9.0 \times 10^{-1}$  to  $9.5 \times 10^{-1}$ ; e.g., Figure 7). With the very

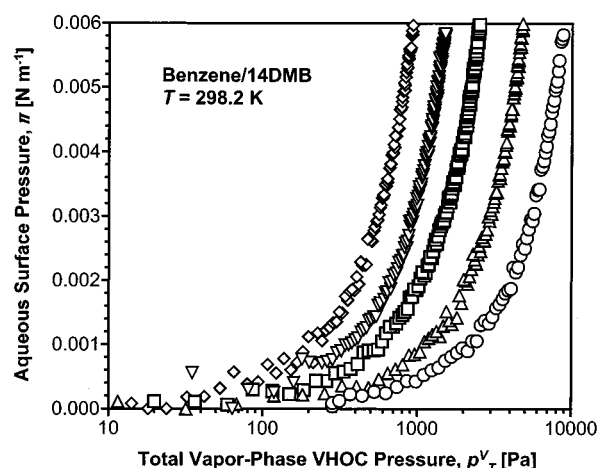


**Figure 3.** Measured aqueous solution surface pressure  $\pi$  as a function of total vapor-phase VHOC pressure  $p_T^V$  isotherms at 298.2 K for the benzene/14DMB solute pair. Mean 14DMB vapor-phase mole ratio  $z_2^V = 1$  ( $\diamond$ ),  $z_2^V = 6.76 \times 10^{-1}$  ( $\nabla$ ),  $z_2^V = 3.48 \times 10^{-1}$  ( $\square$ ),  $z_2^V = 1.20 \times 10^{-1}$  ( $\triangle$ ), and  $z_2^V = 0$  ( $\circ$ ).

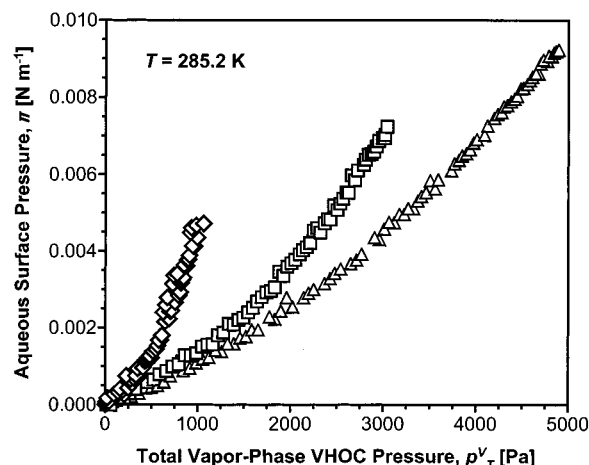


**Figure 4.** Measured aqueous solution surface pressure  $\pi$  as a function of total vapor-phase VHOC pressure  $p_T^V$  isotherms at 285.2 K for benzene/VHOC2 solute pairs at similar mean vapor-phase mole ratios. Mean MB vapor-phase mole ratio  $z_2^V = 1.32 \times 10^{-1}$  ( $\diamond$ ), mean 14DMB vapor-phase mole ratio  $z_2^V = 9.3 \times 10^{-2}$  ( $\square$ ), and mean 135TMB vapor-phase mole ratio  $z_2^V = 9.9 \times 10^{-2}$  ( $\triangle$ ).

good agreement for the other cases considered, it seems a reasonable conclusion that the discrepancies are most probably the result of experimental error in single and/or binary adsorption measurements. Additionally, in the applications of eq 6 to the experimental data, any errors in the single component VOC adsorption measurements are transferred throughout the defined functions for prediction of binary solute behavior.

To briefly note, interface-phase activity coefficients, calculated in terms of the two-suffix Margules equation<sup>9,25</sup> were also considered to account for the noted discrepancy of some experimental data with eq 6. However, the inconsistency of derived parameters among different VHOC pairs and temperatures, the limited number of data points, and the excellent application of the ideal interpretation in the great majority of experimental cases negated further consideration.

From application of eq 6 to the data, it is now possible to relate vapor-phase mole ratios to VHOC mixing at the interface. The derived functions (eq 8) for the five solute pairs are presented in Figure 8 from the 285.2 K data decomposed at  $4 \times 10^{-3}$  N m<sup>-1</sup>. The distinct trends as a function of solute type

TABLE 3: Measured Isotherm Characteristics and Results of Equation 13 Interpolations for Single VHOC Experiments

VHOC	$T$ [K]	$n^a$	fraction measured $\frac{p_{V,\text{pure}}}{p_{i,\text{max}}} \frac{p_{V,\text{pure}} - 1}{p_{i,\text{sat}}}$	eq 13 parameters		$R^{2b}$
				$a^0 \times -10^{-5} [\text{m}^2 \text{mol}^{-1}]$	$c \times 10^{-1} [\text{unitless}]$	
B <sup>c</sup>	285.2	277	1.06	0.705	1.37	0.998
	291.2	281	1.05	1.29	1.43	0.997
	298.2	237	0.905	1.78	1.46	1.00
MB	285.2	84	0.926	1.10	1.25	0.996
	291.2	102	0.944	0.602	1.30	0.998
	298.2	243	0.957	1.80	1.33	0.994
12DMB	285.2	57	1.05	2.45	1.18	0.995
	291.2	82	1.00	2.11	1.20	0.994
	298.2	95	1.07	2.39	1.26	0.992
13DMB	285.2	100	0.975	2.52	1.19	0.994
	291.2	96	1.00	1.72	1.20	0.998
	298.2	101	0.925	1.98	1.26	0.994
14DMB	285.2	76	0.951	2.13	1.18	0.995
	291.2	92	0.893	1.49	1.22	0.987
	298.2	162	0.983	1.18	1.23	0.997
135TMB	285.2	96	0.950	3.84	1.09	0.985
	291.2	92	0.969	2.96	1.12	0.987
	298.2	169	0.988	2.84	1.17	0.989

<sup>a</sup> Coefficient of determination. <sup>b</sup> Number of data points. <sup>c</sup> B  $\equiv$  benzene.

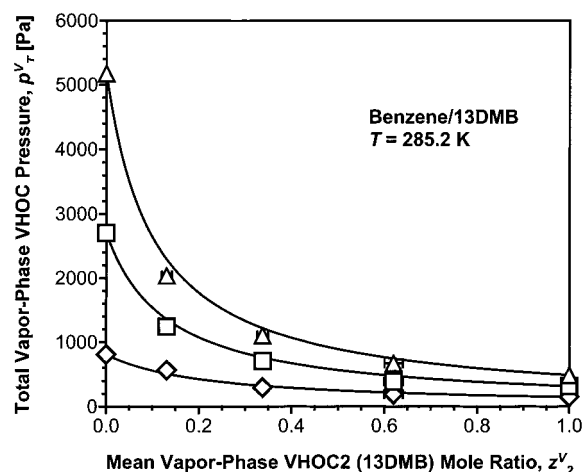


**Figure 5.** Total vapor-phase VHOC pressure  $p_T^V$  as a function of mean vapor-phase VHOC2 mole ratio  $z_2^V$  at 285.2 K for the benzene/13DMB solute pair. Aqueous solution surface pressure  $\pi = 1 \times 10^{-3} \text{ N m}^{-1}$  ( $\diamond$ ),  $\pi = 3 \times 10^{-3} \text{ N m}^{-1}$  ( $\square$ ), and  $\pi = 7 \times 10^{-3} \text{ N m}^{-1}$  ( $\triangle$ ). Error bars (barely visible behind symbols) represent one standard deviation for the mean vapor-phase mole ratios ( $z_1^V$  and  $z_2^V$ ). Solid curve represents application of eq 6.

are evident, with very similar results derived for the three dimethylbenzene isomers. Inspection reveals that for any given vapor-phase VHOC2 mole ratio, the interface phase has a greater solute mole ratio with respect to that methyl-substituted benzene component. The relative degree of this interface-phase enrichment is also greater as the molecular size of component 2 increases with respect to benzene. In most cases, no discernible differences as a function of surface pressure or temperature considered were noted for the application of eq 8.

As the proceeding discussion and analyses have significant similarity to the Raoult's law definition of vapor–liquid equilibrium (VLE), it was worthwhile to compare mixing in the idealized organic liquid phase (i.e., no air/water present) to that at the vapor/water interface for given vapor-phase mole fractions and mole ratios, respectively. As mentioned previously, mixing in the organic liquid phase was assumed ideal for the considered compounds.<sup>1,26,27</sup> This was validated by inspection of vapor–liquid equilibrium data compiled for the benzene/MB, benzene/13DMB, benzene/14DMB systems,<sup>28</sup> and consideration of Scatchard–Hildebrand regular solution theory for

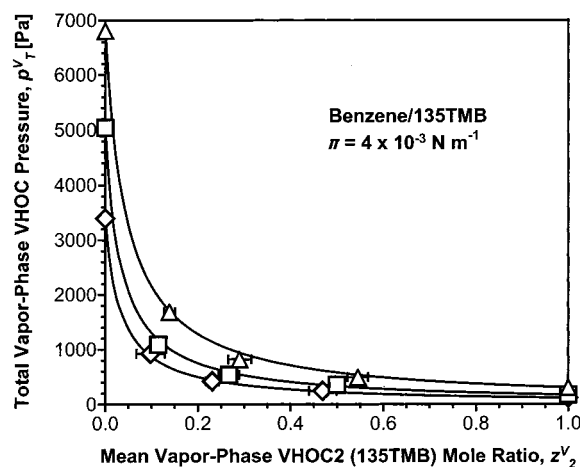


**Figure 6.** Total vapor-phase VHOC pressure  $p_T^V$  as a function of mean vapor-phase VHOC2 mole ratio  $z_2^V$  at  $4 \times 10^{-3} \text{ N m}^{-1}$  for the benzene/135TMB solute pair. Temperature  $T = 285.2 \text{ K}$  ( $\diamond$ ),  $T = 291.2 \text{ K}$  ( $\square$ ), and  $T = 298.2 \text{ K}$  ( $\triangle$ ). Error bars represent one standard deviation for the mean vapor-phase mole ratios ( $z_1^V$  and  $z_2^V$ ). Solid curve represents application of eq 6.

the benzene/12DMB and benzene/135TMB pairs.<sup>25</sup> Vapor-phase/organic liquid-phase equilibrium was defined using exact application of Raoult's law:

$$x_2^L = p_{1,\text{sat}}^{\text{V,pure}} / [p_{1,\text{sat}}^{\text{V,pure}} + p_{2,\text{sat}}^{\text{V,pure}} / y_2^V - p_{2,\text{sat}}^{\text{V,pure}}] \quad (15)$$

where  $x_2^L$  is the organic liquid-phase mole fraction of component 2 and  $y_2^V$  is the vapor-phase mole fraction of component 2. Results from eq 15 for the benzene/MB, benzene/12DMB, and benzene/135TMB pairs at 291.2 K (solid curves) are compared to results from eq 8 at constant surface pressure of  $4 \times 10^{-3} \text{ N m}^{-1}$  (dashed curves) in Figure 9. The similarity suggests that the solute–solute interactions occurring at the interface are similar to that encountered in bulk organic liquid. Differences between the two curves may be attributable to experimental error, but also may reflect interface-phase solute–water interactions. Further experimental consideration is necessary to address these interpretations. However, the understanding that vapor-phase/organic liquid-phase equilibrium and vapor-phase/interface-phase equilibrium define similar mole ratio (fraction) relationships offers a potential means to predict vapor-phase/

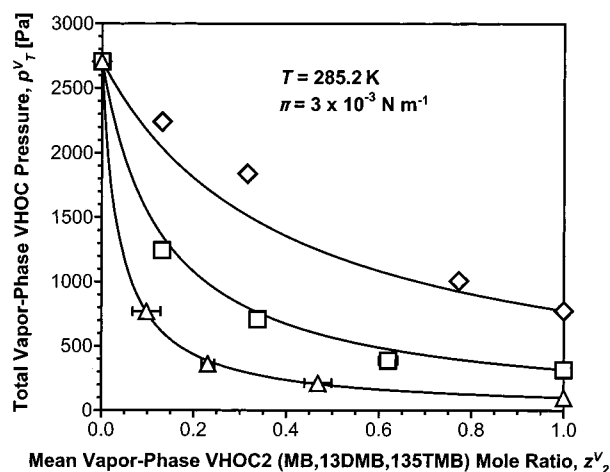


**Figure 7.** Total vapor-phase VHOC pressure  $p_T^V$  as a function of mean vapor-phase VHOC2 mole ratio  $z_2^V$  at  $3 \times 10^{-3} \text{ N m}^{-1}$  and 285.2 K for the solute pairs: benzene/MB ( $\diamond$ ), benzene/13DMB ( $\square$ ), and benzene/135TMB ( $\triangle$ ). Error bars represent one standard deviation for the mean vapor-phase mole ratios ( $z_1^V$  and  $z_2^V$ ). Solid curve represents application of eq 6.

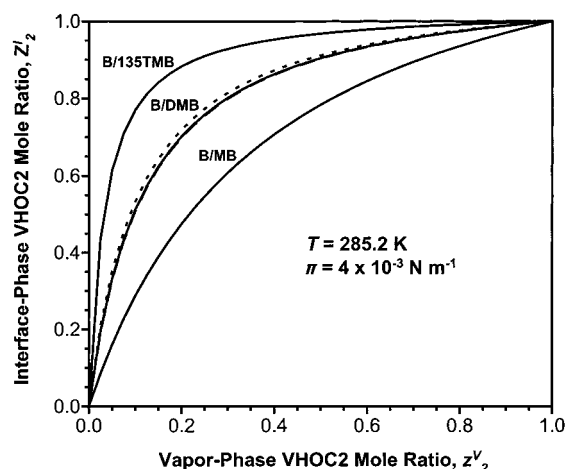


**Figure 8.** Interface-phase VHOC2 mole ratio  $Z_2^I$  as a function of vapor-phase VHOC2 mole ratio  $z_2^V$  at  $4 \times 10^{-3} \text{ N m}^{-1}$  and 285.2 K for the solute pairs: benzene/MB, benzene/12DMB (dotted curve), benzene/13DMB (dashed curve, barely visible), benzene/14DMB, and benzene/135TMB. DMB denotes dimethylbenzene isomers.

interface-phase mixing, specifically nonideal mixing, of other VHOCs based on more readily available VLE data.

**Interface-Phase Adsorption.** Total relative solute interface excess as a function of total vapor-phase VHOC pressure was approximated from experimental surface pressure isotherms using eqs 10–14; results for the benzene/14DMB solute pair at 291.2 K are illustrated in Figure 10 (open symbols, presented semilogarithmically). As noted for the surface pressure isotherms, distinct separation between relative excess isotherms as a function of mole ratio is evident, with greater interface VHOC adsorption for a given  $p_T^V$  as  $z_2^V$  increases (consistent with all current relative interface excess isotherms). The absence of discontinuities in isotherm shape as a function of vapor-phase composition suggest complete miscibility of the VHOC components in the interface-phase.<sup>6,18,29</sup>

Total relative solute interface excess for binary VHOC adsorption was determined theoretically from application of eq 9 to single solute interface excess derived from experiment. Values were determined at  $1 \times 10^{-3} \text{ N m}^{-1}$  intervals for each mixture pair, temperature, and measured mean vapor-phase

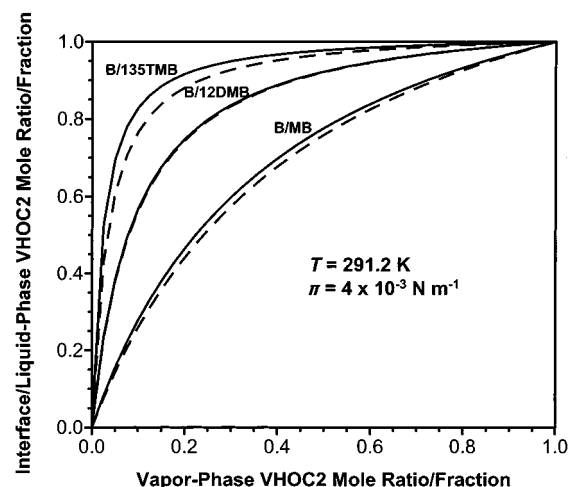


**Figure 9.** Interface-phase VHOC2 mole ratio  $Z_2^I$  (dashed curve) as a function of vapor-phase VHOC2 mole ratio  $z_2^V$  at  $4 \times 10^{-3} \text{ N m}^{-1}$  and 291.2 K and organic liquid-phase VHOC2 mole fraction  $x_2^L$  as a function of vapor-phase VHOC2 mole fraction  $y_2^V$  (from Raoult's law, solid curve) for the solute pairs: benzene/MB, benzene/12DMB, and benzene/135TMB.

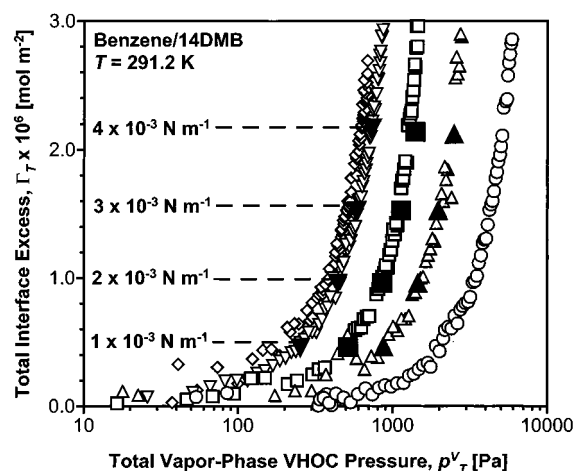


**Figure 10.** Total relative solute interface excess  $\Gamma_T$  as a function of total vapor-phase VHOC pressure  $p_T^V$  isotherms at 291.2 K for the benzene/14DMB solute pair. Mean 14DMB vapor-phase mole ratio  $z_2^V = 1$  ( $\diamond$ ),  $z_2^V = 6.66 \times 10^{-1}$  ( $\nabla$ ),  $z_2^V = 3.23 \times 10^{-1}$  ( $\square$ ),  $z_2^V = 1.25 \times 10^{-1}$  ( $\triangle$ ), and  $z_2^V = 0$  ( $\circ$ ). Filled symbols represent determinations based on eq 9 with associated values of constant surface pressure.

solute mole ratio (Table 2). Results for the benzene/14DMB solute pair at 291.2 K are depicted in Figure 10 (filled symbols) and illustrate the good agreement between experimental and theoretical determination of the binary VHOC adsorption currently considered. For all systems analyzed, mean agreement between results is within 15%, excellent in light of the strong nonlinearity of the measured total relative solute interface excess isotherms and the disparate vapor-phase solute pressure dependence of the single VHOC isotherms as a function of solute type.

## Conclusions

The presented application of pendant drop tensiometry and gas chromatographic analysis in conjunction with a dynamic adsorption protocol has provided the first analysis of the binary vapor-phase/interface-phase mixing for VHOCs at the vapor/water interface. It is apparent that adsorption behavior at the interface is well defined by an ideal mixing framework and that

partial relative solute interface excess can be determined from single-component relative interface excess (cf. 5,7) for the VHOCs, temperatures, and pressures considered. Additionally, vapor-phase/interface-phase mole ratio relationships are very similar to vapor-phase/organic liquid-phase mole fraction relationships derived from Raoult's law, suggesting similar interaction of mixed solutes in the interface phase and bulk organic liquid phase. While ideal systems have currently only been considered, it is our intention to further this analysis, in terms of precision and scope, to VHOC systems with known nonideality in bulk organic liquid-phase mixtures.

**Acknowledgment.** The project described was supported by grant number 2 P42 ESO4940-11 from the National Institute of Environmental Health Sciences, NIH, with funds from U.S. EPA. Its contents are solely the responsibility of the authors and do not necessarily represent the official views of the NIEHS, NIH, and EPA. The authors are extremely appreciative of comments and suggestions provided by Mr. Timothy Corley (University of Arizona), Dr. Ingrid Padilla (Gregory L. Morris & Assoc.), Dr. Sriniraghavan (U. of Arizona), Mr. Jeffery Silva (Duke Engineering & Services), and the anonymous reviewers.

## References and Notes

- (1) Banerjee, S. *Environ. Sci. Technol.* **1984**, *18*, 587.
- (2) Dickhut, R. M.; Armstrong, D. E.; Andren, A. W. *Environ. Toxicol. Chem.* **1991**, *10*, 881.
- (3) Lesage, S.; Brown, S. J. *Contam. Hydrol.* **1994**, *15*, 57.
- (4) Valsaraj, K. T. *Water Res.* **1994**, *28*, 819.
- (5) Myers, A. L.; Prausnitz, J. M. *AIChE J.* **1965**, *11*, 121.
- (6) Iyoda, H.; Aratono, M.; Motomura, K. *J. Colloid Interface Sci.* **1996**, *178*, 53.
- (7) Radke, C. J.; Prausnitz, J. M. *AIChE J.* **1972**, *18*, 761.
- (8) Rosen, M. J.; Hua, X. Y. *J. Colloid Interface Sci.* **1982**, *86*, 164.
- (9) Smith, J. M.; Van Ness, H. C. *Introduction to Chemical Engineering Thermodynamics*, 4th ed.; McGraw-Hill: New York, 1987.
- (10) Todoroki, N.; Tanaka, F.; Ikeda, N.; Aratono, M.; Motomura, K. *Bull. Chem. Soc. Jpn.* **1993**, *66*, 351.
- (11) Villeneuve, M.; Sakamoto, H.; Minamizawa, H.; Ikeda, N.; Motomura, K.; Aratono, M. *J. Colloid Interface Sci.* **1997**, *194*, 301.
- (12) Aveyard, R. Adsorption at the Air/Liquid, Liquid/Liquid, and Solid/Liquid Interfaces. In *Surfactants*; Tadros, Th. F., Ed.; Academic Press: London, 1984.
- (13) Jones, D. C.; Ottewill, R. H. *J. Chem. Soc.* **1955**, 4067.
- (14) Kemball, C.; Rideal, E. K. *Proc. R. Soc. London* **1946**, *A187*, 53.
- (15) Volmer, M. Z. *Phys. Chem.* **1925**, *115*, 263.
- (16) Aratono, M.; Kanda, T.; Motomura, K. *Langmuir* **1990**, *6*, 843.
- (17) Chattoraj, D. K.; Birdi, K. S. *Adsorption and the Gibbs Surface Excess*; Plenum: New York, 1984.
- (18) Motomura, K.; Kanda, T.; Abe, K.; Todoroki, N.; Ikeda, N.; Aratono, M. *Colloids Surf.* **1992**, *67*, 53.
- (19) Daubert, T. E.; Danner, R. P. *Physical and Thermodynamic Properties of Pure Chemicals: Data Compilation*; Hemisphere Publishing Co.: New York, 1989.
- (20) Bruant, R. G., Jr.; Conklin, M. H. *J. Phys. Chem. B* **2000**, *104*, 11146.
- (21) Bruant, R. G., Jr.; Conklin, M. H. *Environ. Sci. Technol.* **2001**, *35*, 362.
- (22) Cheng, P.; Li, D.; Boruvka, L.; Rotenberg, Y.; Neumann, A. W. *Colloids Surf.* **1990**, *43*, 151.
- (23) Cheng, P.; Neumann, A. W. *Colloids Surf.* **1992**, *62*, 297.
- (24) Garrett, P. R. *J. Chem. Soc., Faraday Trans.* **1976**, *72*, 2174.
- (25) Prausnitz, J. M.; Lichtenthaler, R. N.; Gomes de Azevedo, E. *Molecular Thermodynamics of Fluid-Phase Equilibria*, 3rd ed.; Prentice Hall: Upper Saddle River, New Jersey, 1999.
- (26) Leinonen, P. J.; Mackay, D. *Can. J. Chem. Eng.* **1973**, *51*, 230.
- (27) Mackay, D.; Shiu, W. Y.; Maijanen, A.; Feenstra, S. J. *Contam. Hydrol.* **1991**, *8*, 23.
- (28) Gmehling, J.; Onken, U.; Arlt, W. *Vapor-Liquid Equilibrium Data Collection: Aromatic Hydrocarbons*; DECHEMA: Flushing, New York, 1977; Vol. 1; Part 7.
- (29) Pagano, R. E.; Gershfeld, N. L. *J. Phys. Chem.* **1972**, *76*, 1238.